Build-up and relaxation of membrane fouling deposits produced during crossflow ultrafiltration of casein micelle dispersions at 12 °C and 42 °C probed by in situ SAXS

Floriane Doudiès, Maksym Loginov, Nicolas Hengl, Mohamed Karrouch, Nadine Leconte, Fabienne Garnier-Lambrouin, Javier Pérez, Frédéric Pignon, Geneviève Gésan-Guiziou

Journal of Membrane Science 618 (2021) 118700

Contents lists available at ScienceDirect

Journal of Membrane Science

journal homepage: http://www.elsevier.com/locate/memsci

Build-up and relaxation of membrane fouling deposits produced during crossflow ultrafiltration of casein micelle dispersions at 12 °C and 42 °C probed by *in situ* SAXS

Floriane Doudiès [a,b], Maksym Loginov [a], Nicolas Hengl [b], Mohamed Karrouch [b], Nadine Leconte [a], Fabienne Garnier-Lambrouin [a], Javier Pérez [c], Frédéric Pignon [b,**], Geneviève Gésan-Guiziou [a,*]

[a] STLO, INRAE, Institut Agro, 35042, Rennes, France
[b] Univ. Grenoble Alpes, CNRS, Grenoble INP (Institute of Engineering Univ. Grenoble Alpes), LRP, F-38000, Grenoble, France
[c] Beamline SWING, Synchrotron SOLEIL, 91192, Gif-sur-Yvette, France

ARTICLE INFO

Keywords:
Milk filtration
Membrane fouling
Reversibility of compression
Relaxation
Swelling

ABSTRACT

Skim milk filtration is performed either at low or high temperature. However, there is still a lack of knowledge concerning the influence of temperature on membrane fouling. We used *in situ* small-angle X-ray scattering (SAXS) to study external membrane fouling during crossflow ultrafiltration of milk protein (casein micelle) dispersions at 12 °C and 42 °C. Casein micelle concentration distribution was measured in the concentration polarization layer and the deposit in a three-step filtration experiment that consisted of (i) fouling development step (with applied pressure and average cross-flow velocity fixed at 110 kPa and 3.1 cm s^{-1}, respectively), (ii) pressure relaxation step (with pressure reduced to 10 kPa), and (iii) deposit erosion step (with crossflow velocity increased to 15.6 cm s^{-1}).

Despite a higher average filtrate flux obtained at 42 °C, filtration at 42 °C resulted in the formation of a thicker and more concentrated deposit than filtration at 12 °C. At both temperatures studied, subsequent pressure relaxation resulted in deposit swelling, which was more intense in the less-compressed external part of the deposit. Deposit swelling rate was significantly higher at 42 °C than at 12 °C. The swelled deposit obtained at 42 °C was more eroded by the crossflow compared to the poorly swelled deposit obtained at 12°. This suggests that deposit formation and compression were more reversible at 42 °C than at 12 °C.

1. Introduction

1.1. The membrane fouling problem in low- and high-temperature milk filtration

Milk filtration became an essential dairy industry process with the development of membrane technology, first with tubular ceramic membranes and, later, spiral-wound polymer membranes [1]. For example, microfiltration is used to separate casein micelles from serum proteins, and ultrafiltration is used to concentrate the milk proteins. Milk is filtered at high (50–55 °C) or low (9–15 °C) temperatures to curb the bacterial growth that leads to milk spoilage and equipment contamination [2]. High-temperature filtration generally uses ceramic membranes, which although expensive are preferred for their better cleanability and durability, while low-temperature filtration uses cheaper but less durable polymeric membranes.

Membrane fouling degrades the efficiency of both high- and low-temperature milk filtration, but it is apparently inevitable given that the composition of milk can give rise to different foulant–foulant and membrane–foulant interactions [2]. Along with bacterial development, membrane fouling obliges to interrupt a milk filtration cycle (which generally lasts about 6–8 h with ceramic membrane filtration and up to 15 h with polymeric membrane filtration) for 2–3 h of cleaning operations that include several physical and chemical membrane cleaning steps [1,3,4]. A recent environmental performance assessment of

Abbreviations: E, erosion step; F, filtration step; R, pressure relaxation step; SAXS, small-angle X-ray scattering.

* Corresponding author.
** Corresponding author.
E-mail addresses: frederic.pignon@univ-grenoble-alpes.fr (F. Pignon), genevieve.gesan-guiziou@inrae.fr (G. Gésan-Guiziou).

https://doi.org/10.1016/j.memsci.2020.118700
Received 9 July 2020; Received in revised form 25 August 2020; Accepted 31 August 2020
Available online 5 September 2020

Nomenclature

Greek

μ	filtrate viscosity (Pa s)
υ	voluminosity of casein micelles (ml g^{-1})
Π	local osmotic pressure in the deposit (Pa)
τ_w	wall shear stress (Pa)
ϕ	volume fraction of casein micelles (dimensionless)
ϕ_{eff}	effective volume fraction of casein micelles (dimensionless)
ϕ_{gs}	volume fraction of casein micelles at the gel–sol transition (dimensionless)
ϕ_{sg}	volume fraction of casein micelles at the sol–gel transition (dimensionless)

Latin

c	casein concentration (g l^{-1})
c_0	casein concentration in bulk (g l^{-1})
h_g	gel thickness (μm)
I	intensity of the scattered X-ray beam (arbitrary units)
I_{tr}	intensity of the transmitted X-ray beam (arbitrary units)
J	filtrate flux (m s^{-1})
J_L	average filtrate flux along the membrane at the filtration stage (m s^{-1})
L	length of the filter channel and membrane (cm)
m_{ex}	excess weight of casein in the concentration polarization layer and deposit (g m^{-2})
q	scattering vector (nm^{-1})
R	average hydraulic resistance of the membrane (m^{-1})
R_f	average hydraulic resistance of fouled membrane (m^{-1})
R_m	average hydraulic resistance of clean membrane (m^{-1})
R_r	average hydraulic resistance of rinsed membrane (m^{-1})
T	temperature (°C)
t	time (s)
t_E	time of the erosion step (s)
t_F	time of the filtration step (s)
t_R	time of the pressure relaxation step (s)
TMP	transmembrane pressure (Pa)
v	average crossflow velocity (cm s^{-1})
x	horizontal distance from the entrance to the filter channel (cm)
z	vertical distance from the membrane surface (μm)

current cleaning protocols found that they demand excessive amounts of time, energy, water and chemicals [5]. Fouling control and optimization of membrane cleaning are therefore ongoing challenges for the dairy industry that require research into fouling mechanisms, foulant–foulant and foulant–membrane interactions (e.g. properties of fouling deposits), and conditions governing fouling development and removal.

Despite a large body of research into membrane fouling and membrane cleaning in milk filtration (e.g. Refs. [2–4,6–28]), they are indeed not sufficiently studied. It is difficult to analyze and explain the published data on milk filtration: for example, different conclusions can be found about the role of transmembrane pressure ([10] and [6,7,13,17,29–34]) and temperature ([12,19] and [33]) in membrane fouling; even the qualitative composition of the fouling layer is under discussion ([13,25,31] and [21,35]), etc.

One reason for this uncertainty is that many of previous studies have focused on parameter averages to characterize membrane fouling (average filtrate flux and membrane resistance, e.g. Ref. [12]). Only few researchers studied local membrane fouling in milk filtration: e.g. Refs. [10,80,82,83] measured local fouled membrane resistance, while [50] directly characterized local deposit layer (also, there were reports on characterization of local membrane fouling by milk with the help of complex optical methods [3,15,81]). Moreover, very different flux reducing effects can occur during membrane filtration: for example, it can be expected that microfiltration with more open porous membranes will be affected more by pore blocking than ultrafiltration. Unfortunately, the membrane fouling mechanism is not always discussed or validated. Also, there are other difficulties of reaching sufficient precision in the data presentation and analysis (as detailed in Appendix). Therefore, apparent contradictions between conclusions made in different studies on the basis of raw data comparison should not be discussed as conflicting, but rather yielded by difference (usually, undefined) in fouling mechanisms, operating conditions or properties of studied fluids. It can be expected that these contradictions can be avoided, if membrane fouling phenomena are discussed in addition to basic filtration data. Therefore, rigorous characterization of membrane fouling needs to consider the conditions governing fouling development, the type of fouling and its properties (e.g. spatio-temporal evolution of the concentration polarization layer and deposit), and the kinetics of fouling removal.

1.2. Role of casein micelle deposits in membrane fouling

The present study is focused on characterizing the local membrane fouling by deposit produced during the ultrafiltration of casein micelle dispersions. Casein micelles are the main colloidal constituents of skim milk. According to Ref. [31], during skim milk filtration, casein micelles play a central role in "irreversible membrane fouling" (where "irreversibility" is defined according to Refs. [7,76]) via the formation of "irreversible" casein micelle deposit under critical filtration conditions (in line with previous theoretical considerations [36] and further experimental findings [37]).

Casein micelles represent about 80 wt% of milk proteins. They are roughly spherical colloidal agglomerates with diameter ranging from 50 nm to 500 nm and an average diameter of about 150–200 nm [38,84–86], whereas other milk proteins are dissolved in serum as monomers or dimers. The micelles are core-shell-type particles composed of assemblies of α_{s1}-, α_{s2}- and β-casein molecules connected with nanoparticles of calcium phosphate and covered with a κ-casein brush lending them stability against aggregation. Casein micelles are soft colloids, which means they are highly porous, deformable, and can shrink under compressive pressure and re-swell after pressure release [39,40].

Concerning the properties of casein micelles at high concentrations [41–43], studied osmotic compression of casein micelle dispersions and demonstrated that casein micelles form gels when the critical sol–gel transition concentration and the corresponding critical osmotic pressure are exceeded. Once the compressive pressure is released, these gels swell and redisperse over the course of time. In highly-compressed gels, concentration of gel–sol transition is lower than that sol–gel transition [40] (this demonstrates partial irreversibility of compression of casein micelles gels obtained via osmotic compression). In the later study on membrane filtration of casein micelle dispersions [37] it was confirmed that a critical minimal transmembrane pressure is required in order to obtain persistent membrane fouling (that was explained by deposit formation). The results of dynamic compression of fouled membranes also suggested that the deposit of casein micelles is reversibly compressible (i.e. it gets compressed and re-swells after the change of applied pressure [37] similarly to gels of casein micelles obtained via osmotic compression [40]).

Besides, a series of work from the Technical University of Munich [8,

11,32,33] systematically demonstrated that removal of fouling during membrane rinsing after filtration of skim milk is a continuous process. It was also suggested that the kinetics of fouling removal is related to deposit compression (which slows down fouling removal) and diffusion of foulant into the bulk (which was assumed to be the mechanism of fouling removal). The evidence from Refs. [8,11,32,33] and [37,40] suggests that deposit swelling must take place in parallel with redispersion (diffusion, in terms of [8]) and thus play a role in fouling removal.

Therefore, in the case of formation and removal of casein micelle deposit, meaningful discussion of fouling should be based on quantitative characterization of deposit properties, i.e. concentration profile, permeability, compressibility, reversibility of compression, and cohesiveness (as previously done for gels obtained by osmotic compression in Refs. [41,42] and dead-end filtration in Ref. [44]).

1.3. Influence of temperature on casein micelles and fouling deposits

Decreasing temperature (<12 °C) results in the partial release of β-casein and calcium phosphate from casein micelles into the serum phase [45]. It also increases casein micelle voluminosity υ (the ratio of particle volume to particle dry weight): according to Refs. [46,47], decreasing the temperature from 70 °C to 5 °C increases υ from 3.5 ml g^{-1} to 5.0 ml g^{-1}. These temperature-related phenomena may be important for milk filtration due to their possible influence on the membrane fouling. For example, it was demonstrated that compressibility of casein micelles dispersions obtained by compression at constant osmotic pressure significantly changes in the temperature range 7–20 °C (i.e. at constant osmotic pressure, casein micelle concentration increases with temperature) [41]. Therefore, temperature can influence the compressibility of casein micelle deposits on the membrane surface.

However, to the best of the authors' knowledge, the influence of filtration temperature on the properties (permeability, compressibility, reversibility of compression, cohesiveness) of casein micelles deposits produced in crossflow mode has never been investigated. Here we premise that this influence can be characterized via proper analysis of local solid concentration distribution in deposits obtained at different filtration temperatures. Previously, it was demonstrated that the required concentration distribution for casein micelles (as well as other colloids) can be measured *in situ* with a spatial resolution of tens of microns via small-angle X-ray scattering (SAXS) [48–50]. These previous studies used specific X-ray-adapted crossflow filtration cells to capture the time-course and spatial evolutions of casein micelle concentrations during the process under controlled crossflow, transmembrane pressure (TMP) and temperature. Using these purpose-designed filtration cells together with a highly collimated X-ray beam, it was managed to capture this time-resolved spatial information and its process time-course kinetics within the concentration polarization layers and deposits, in the vicinity of the membrane surface at distances down to a few hundred micrometers with a precision of 20 μm.

In the present article we combined data on local deposit concentration obtained via *in situ* SAXS–filtration method with the filtration flux measurements in a multi-step filtration experiment set up to vary TMP and crossflow velocity to shed light on the influence of filtration temperature on the formation and reversibility of casein micelle deposits.

The experiments were carried out at 12 °C and 42 °C (close to typical industry temperatures for skim milk filtration) using casein micelles dispersed in skim milk ultrafiltrate. SAXS–filtration data were analyzed, deposit removal was described, and the relationship between average (hydraulic resistance of fouled membrane) and local (deposit properties) data was discussed.

2. Experimental

2.1. Casein micelle dispersions

Casein micelle dispersions were prepared from casein micelle powder and milk ultrafiltrate (UF permeate). Casein micelle powder Promilk 852B was provided by Ingredia (Arras, France) and was obtained by microfiltration of pasteurized skim milk with a membrane pore size of 0.1 μm. UF permeate was prepared at the STLO laboratory by ultrafiltration of a fresh skim milk at 12 °C through a membrane with a nominal molecular weight cut-off of 5 kDa. Thiomersal (0.02 wt%) and sodium azide (0.05 wt%) (both from Sigma-Aldrich, USA) were added to the UF permeate as preservatives. Detailed compositions of the micellar casein powder and UF permeate can be found in Supplementary material.

Casein micelle dispersions were prepared by thoroughly mixing casein micelle powder with UF permeate for 15 h at 35 °C. According to the literature [51,52], this method allows to recover the main properties of casein micelles. Dynamic light scattering analysis confirmed that the casein micelles dispersions had a particle size distribution from 50 nm to 450 nm with an average diameter of 130 nm, i.e. similar to native casein micelles. pH of the dispersions was 6.7 ± 0.1 at 20 °C, which is the pH value of fresh skim milk.

The dispersions were then stored at 4 °C and used within 24 h after preparation. Before experiments, dispersions were warmed up in a water bath and then kept at the desired temperature (12 °C or 42 °C) for 30 min in order to complete the temperature-induced transformations of casein micelles.

2.2. In situ SAXS crossflow ultrafiltration rig

Crossflow filtration experiments were performed in a SAXS–ultrafiltration cell (Fig. 1), and local casein micelle concentration in the fouling layer was obtained by *in situ* SAXS method as described elsewhere [49].

The crossflow filtration cell ('5' in Fig. 1) was made of transparent polycarbonate; it was composed from upper (retentate) and lower (permeate) hollow parts with the flat polymeric filtration membrane sandwiched between them. The membrane was supported by a perforated stainless steel plate. The retentate channel has a length of $L = 100$ mm (in the crossflow direction), height 8 mm (perpendicular to the membrane surface) and width 4 mm. Membrane surface area was 4×10^{-4} m^2. Motorized stages ('10' in Fig. 1b) served to move the cell in x and z directions and to rotate it around the x axis.

During filtration, the feed dispersion was pumped ('3' in Fig. 1a; LF-series Mono Pump) from a pressurized thermostated vessel ('2' in Fig. 1a; Millipore 5 L, Merck Millipore, France) to the filtration cell. Crossflow velocity v was continuously measured using a magnetic flowmeter ('7' in Fig. 1a; Optiflux 6300C, Krohne, France). Pressure was applied to the rig via a purified compressed air system ('1' in Fig. 1a) and monitored by two pressure gauges ('4' and '4'' in Fig. 1a; FP 110 FGP Sensors & Instrument, France) at the inlet and outlet of the filtration cell. Average filtrate flux J_L was monitored by measuring the filtrate weight to an accuracy of 1 mg using an electronic balance ('8' in Fig. 1a; PB 303-S/FACT, Mettler Toledo, France).

Temperature of retentate was maintained by a thermostatic bath (Eco Silver RE 620 SW, Lauda, Germany) and continuously verified by two sensors (YC-747D with type-K thermocouples, Yu Ching technology, Taiwan) at both inlet and outlet of the filtration cell.

2.3. Filtration protocol

Filtration experiments were conducted at 12 °C and 42 °C with casein micelle dispersions at a casein concentration of 49 ± 1 g l^{-1}. Though $T =$ 42 °C (which was highest temperature available with used experimental rig) is lower than $T =$ 50–55 °C (which is industrially common for high temperature milk filtration), it is sufficiently high as compared to $T =$

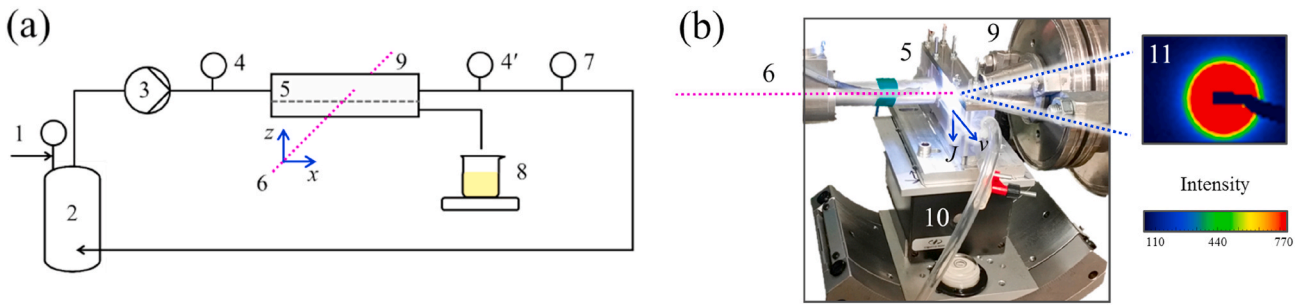

Fig. 1. *In situ* SAXS–ultrafiltration experiment: (a) ultrafiltration rig, (b) *in situ* SAXS analysis. The rig comprises: 1 – compressed air source, 2 – pressurized and thermostated vessel with dispersion, 3 – pump, 4 and 4′ – pressure gauges, 5 – crossflow filtration cell, 6 – incident X-ray beam, 7 – magnetic flowmeter, 8 – weighted filtrate, 9 – scattered X-ray beam, 10 – motorized stages, 11 – example of a SAXS pattern. In (b), the long and short blue arrows show direction of crossflow v and filtrate flow J, respectively. (For interpretation of the references to colour in this figure legend, the reader is referred to the Web version of this article.)

12 °C in order to study effects related with temperature dependency of casein micelle properties.

A new polyethersulfone membrane with a nominal molecular weight cut-off of 100 kDa (Orelis Environnement, France) was used in each filtration run. The membranes were soaked in UF permeate for at least 30 min prior to the experiments.

A three step filtration protocol was devised in order to investigate the formation and properties of the casein micelles layer at the membrane surface (Fig. 2).

At the first step of the experiment (filtration, F), TMP at 110 kPa and crossflow velocity v at 3.1 cm s^{-1} were applied and membrane fouling, casein micelle accumulation on the membrane surface and deposit formation were studied during 150 min. At the second step (pressure relaxation, R), TMP was reduced to 10 kPa at the same v, and the deposit relaxation was observed during 45 min. At the third step (erosion, E), v was increased to 15.6 cm s^{-1} for about 10 min in order to study the cohesiveness of the deposit.

Rather low value of cross-flow velocity $v = 3.1$ cm s^{-1} (lower than that applied in industrial milk filtration) was used in order to promote thick deposit formation that enabled analysis of deposit properties and behavior (this approach is frequently applied for *in situ* analysis of membrane fouling by deposit, e.g. Refs. [48–50,70,71,79]). It corresponded to wall shear stress $\tau_w \approx 0.2$ Pa (at 12 °C) and 0.1 Pa (at 42 °C). Details on wall shear stress values and Reynolds number estimates for each experimental step can be found in Supplementary material. Low pressure was applied during the relaxation and erosion steps to avoid membrane rebound from the support and maintain deposit–membrane surface contact.

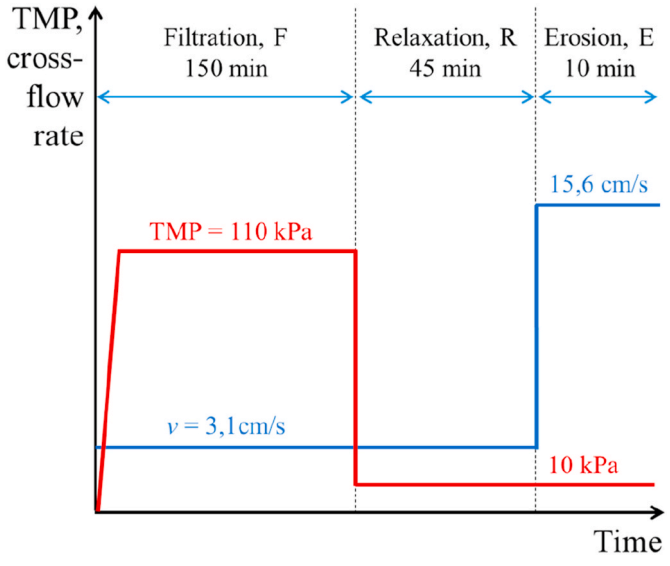

Fig. 2. Schematic of the three-step filtration experiment: filtration is followed by transmembrane pressure relaxation (TMP reduced) and deposit erosion steps (crossflow velocity v increased). Duration of the steps is not to scale.

At the end of each experiment, the filtration cell was disassembled, manually cleaned and rinsed with distilled water, and the fouled membrane was replaced with a new one. Other parts of filtration circuit were rinsed thoroughly with deionized water. Then, 10 L of a 0.5% solution of Ultrasil 25F (Ecolab SNC, France) were recirculated through the filtration rig at 50 °C, TMP = 150 kPa and $v = 50$ cm s^{-1} for 30 min in order to sanitize the equipment, which was finally flushed with deionized water under the same conditions.

pH of the retentate remained constant during the experiments, thus confirming that there was no bacterial contamination of the filtration system and studied dispersions.

2.4. *In situ* SAXS measurements and data analysis

Analysis of local membrane fouling was based on the fact that the intensity of SAXS by casein micelle dispersions is directly proportional to their concentration [48].

SAXS–filtration experiments were performed at the French national synchrotron facility (SOLEIL, Gif-sur-Yvette, France) on the SWING beamline. The 0.1 nm-wavelength incident X-ray beam was collimated to the full width at half maximum 20 μm vertically (z) and 150 μm horizontally (x) using slits (Fig. 3a). A low full width at half maximum in the z axis was essential to get the highly spatially-resolved measurement of local casein concentration distribution normal to the membrane surface (c versus z).

Sample-to-detector distance was fixed at 3 m, which provided a scattering vector q range spanning from 0.05 nm^{-1}–3 nm^{-1}.

Before filtration, the filtration cell was mounted on the motorized stages (Fig. 1b) and the membrane surface was aligned parallel to the incident beam. The membrane surface position was detected at $x = 5$ cm (i.e. at the middle of the filtration cell, where the fouling layer was studied in all experiments) via analysis of transmitted X-ray intensity $I_{tr}(z)$. As explained in Fig. 3a, the membrane surface position $z = 0$ corresponded to the sharp increase of I_{tr}, when the scanning X-ray beam passed from the dense and strongly-absorbing membrane ($z < 0$) to the weakly-absorbing upper part of the filter cell ($z > 0$).

During the experiments, the motorized stage moved the filtration cell vertically (as shown by the up–down arrow in Figs. 3a) and 2D SAXS patterns ('11' in Fig. 1b) measured at different vertical positions of the filter cell (i.e. at different distances from membrane surface z) were recorded on the 2D detector EigerX4M. The patterns obtained were analyzed as described in previous work on *in situ* SAXS filtration [48]. Briefly, scattering patterns were normalized to an absolute intensity scale after applying standard detector corrections and then azimuthally averaged to obtain the dependencies of scattered intensity $I(q)$ (e.g.,

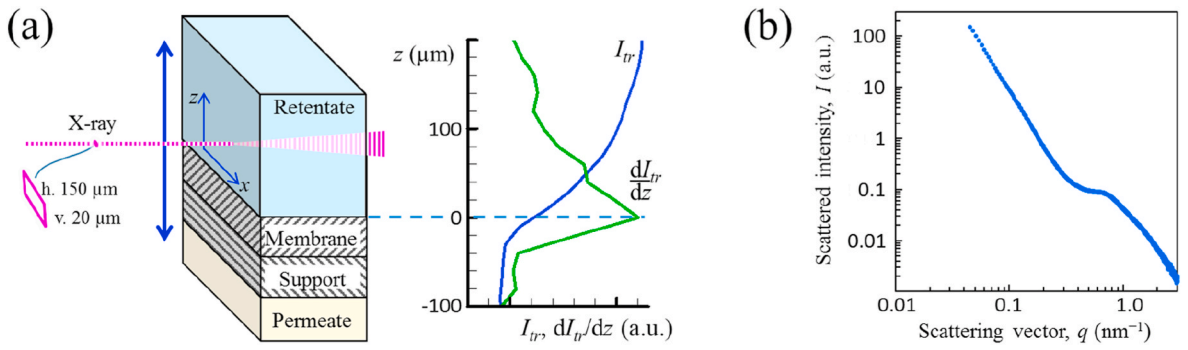

Fig. 3. (a) Side view of *in situ* SAXS measurement (left) and determination of membrane position from the dependency of transmitted X-ray intensity I_{tr} on the vertical position z in the filter cell filled with UF permeate (right): $z = 0$ is assigned to the point where dI_{tr}/dz is maximal; (b) example of $I(q)$ dependency for casein micelle dispersion.

Fig. 3b) using custom software Foxtrot (SWING). These dependencies were obtained for different z values at different timepoints of the filtration experiment. Local concentration of casein micelles was then obtained from $I(q)$ profiles by plotting linear calibration curve c versus I ($q = 1$ nm^{-1}). The calibration curve was obtained in the preliminary experiment, where $I(q)$ patterns were measured for casein micelle dispersions of different known dry matter concentrations c from 2 to 180 g l^{-1}. According to previous studies [48], scattering intensity at $q = 1$ nm^{-1} is unaffected by change in inter-particle interactions and possible anisotropy of the SAXS pattern. The scattered intensity of this range is therefore proportional to number of particles per unit of volume, as already discussed by previous authors [48], and the calibration curve c versus $I(q = 1$ nm$^{-1})$ is linear at least up to $c = 200$ g l^{-1} [48]. Concentration of casein micelles in calibrator dispersions c was obtained via the weight method, as detailed in Supplementary material.

2.5. Analysis of local concentration profiles

Local concentration profiles $c(z)$ (that were obtained at different experiment timepoints t at distance from the filter channel entrance $x =$ 5 cm) are related with accumulation, concentration, deformation and swelling of casein micelles in the fouling layers. The evolution of $c(z)$ was analyzed in order to gain insight into these phenomena.

Casein micelle accumulation in the fouling layer was quantified as an excess weight of casein in the vicinity of the membrane surface m_{ex}, which was calculated from $c(z)$ as

$$m_{ex} = \int_0^{z(c=c_0)} (c(z) - c_0)dz \quad (1)$$

where c_0 is the casein concentration in bulk suspension; $m_{ex} = 0$ in the absence of concentration polarization and increases with increasing concentration polarization.

As casein micelle concentration may result in gel formation [40–43], the thickness of casein micelle gel on the membrane surface h_g was evaluated from $c(z)$ as

$$h_g = z(c = c_{sg}) \quad (2)$$

where c_{sg} is the sol–gel transition concentration of casein micelle dispersions, which was estimated as follows. According to Ref. [41], the sol–gel transition volume fraction of casein micelle dispersions is temperature-independent and equal to $\phi_{sg} = 0.71$. The values of the volume fraction ϕ and concentration c for casein micelles are written as

$$\phi = \upsilon c \quad (3)$$

where υ is the voluminosity of casein micelles (ratio of the volume of a hydrated micelle to its dry weight). According to the literature data, υ is temperature-dependent: $\upsilon = 4.52$ ml g^{-1} and 3.8 ml g^{-1} at 12 °C and 42 °C, respectively (reported in Refs. [46,47]). The casein micelles therefore shrink, and the c_{sg} in casein micelle dispersions increases with increasing temperature. According to the literature data, υ remains constant at least until c reaches c_{sg}. Strictly speaking, the determination of ϕ for $c > c_{sg}$ using Eq. (3) and constant values of υ is not justified. However, as discussed in Ref. [43], ϕ values obtained for $c > c_{sg}$ can be attributed to the effective volume fraction of casein micelles ϕ_{eff}, which serves useful purpose in the analysis of compression and swelling of concentrated casein micelle dispersions. When $\phi_{eff} > 0.71$ (volume fraction of casein micelles in random close-packing [41]), the casein micelles start to deform. Then, $\phi_{eff} > 1$ indicates that the casein micelles are compressed to a lower volume compared to free micelles in a bulk suspension.

Note that the value of $\phi_{sg} = 0.71$ used here was obtained via analysis of the rheological behavior of concentrated casein micelle dispersions prepared by osmotic compression [41], which implies long sample preparation (from days to weeks) in contrast to rapid concentration of micelles on the membrane surface during crossflow filtration. However, the transition from sol-to gel-like behavior as casein micelle dispersions become concentrated was previously explained as the system reaching a critical particle volume fraction without time-dependent particle–particle interactions [43]. Therefore, c_{sg} should be independent of system concentration mode and can thus be used to evaluate the gel thickness during filtration.

2.6. Measurement and analysis of average filtrate flux

Filtrate flux was measured in separate experiments using the same equipment as for the SAXS–filtration experiments, with minor modifications of experimental protocol.

First, the rate of UF permeation at the pressure of 110 kPa was measured, and the hydraulic resistance of clean membrane R_m was calculated.

Second, filtrate flux J_L was measured during filtration of casein micelle dispersions under the same operating conditions as at the first stage of SAXS–filtration (TMP = 110 kPa, $v = 3.1$ cm s^{-1}, Fig. 2). When the steady-state was achieved, the total hydraulic resistance of fouled membrane (i.e. the average value over the membrane length) R_f was calculated.

After the filtration step ($t_F = 150$ min), the membrane was rinsed: the filtration rig was filled with clean ultrafiltrate, and TMP was reduced to 0 kPa for 20 min with crossflow velocity kept at $v = 3.1$ cm s^{-1}. Then, TMP was increased back up to 110 kPa and the rate of clean UF permeation across the rinsed membrane was measured. The average hydraulic resistance of the membrane with remaining (residual) fouling R_r was then calculated (also as an average value over the membrane length).

The values of R_m, R_f and R_r were obtained using Darcy's equation

$$R = TMP / (\mu J) \quad (4)$$

where R is the average hydraulic resistance of the membrane in the filtration cell, J is the measured flux (averaged over the membrane length), and μ is filtrate viscosity (provided in Supplementary material). It should be noted that simple application of Eq. (4) only serves for quantification of the influence of concentration polarization on filtrate flux, it does not allow to differentiate between effects related with increase of osmotic pressure and appearance of hydraulic barrier. It also implies that osmotic pressure of bulk dispersion due to casein micelles is negligible as compared to applied pressure (which is valid for the used values of c_0 and TMP, according to Fig. 8).

These experiments were repeated in duplicate. Average values of R_m, R_f and R_r calculated using Eq. (4) were presented as experimental points, and standard deviations were presented as error bars.

3. Results and discussion

3.1. Casein micelle accumulation during the filtration step

Fig. 4 presents average filtrate flux obtained during crossflow filtration of casein micelle dispersions at 12 °C and 42 °C (both at the constant transmembrane pressure of 110 kPa).

At both temperatures studied, the flux quickly dropped at the beginning of filtration (at $t_F < 10$ min) and then gradually reached the steady-state value (practically constant within the experimental error at $t_F > 50$ min), which was 1.6 times higher at 42 °C than at 12 °C. This result is in the agreement with a number of lab- and pilot-scale studies on low-temperature (6–15 °C) and high-temperature (45–55 °C) crossflow micro- and ultrafiltration of skim milk, where higher filtrate flux was obtained at higher temperature [12,20,21,53–61]. This observation is usually associated with either lower filtrate viscosity (that facilitates liquid permeation across the fouled membrane) [53] or lower retentate viscosity (that reduces the thickness of the concentration polarization layer) [54]. In the authors' opinion, no relevant explanation can be made for the temperature dependence of filtrate flux without the process modelling, which was out of the scope of the present study.

The data presented in Fig. 4 were used to quantify average membrane fouling and determine average fouled membrane resistance R_f (Fig. 5, solid symbols).

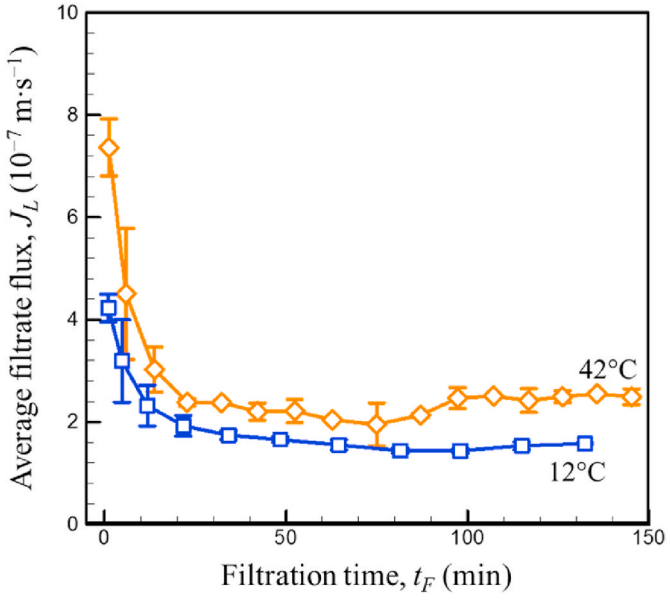

Fig. 4. Average filtrate flux J_L at 12 °C and 42 °C during filtration of casein micelle dispersions ($c_0 = 49 \pm 1$ g l^{-1}) at TMP = 110 kPa and average crossflow velocity $v = 3.1$ cm s^{-1}.

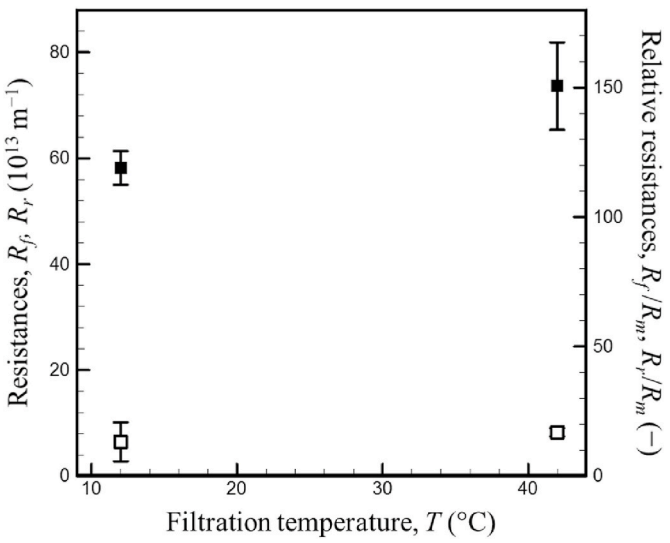

Fig. 5. Average hydraulic resistances during the steady-state stage of filtration R_f (filled symbols) and after the relaxation–rinsing R_r (open symbols): absolute values (left scale) and values relative to clean membrane resistance R_m (right scale). All values are measured at TMP = 110 kPa.

Severe membrane fouling was observed at both studied temperatures ($R_f/R_m > 100$) that significantly exceeded the values typically reported for milk ultrafiltration ($R_f/R_m \approx$ 1–15 [9,10,21,31,62–64]). This can be explained by significantly lower average crossflow velocity and wall shear stress applied here ($v = 3.1$ cm s^{-1}, $\tau_w \approx 0.2$ Pa and 0.1 Pa at 12 °C and 42 °C, respectively), whereas v of the order of 1 m s^{-1} and τ_w of around 100 Pa are required for efficient reduction of fouling during milk filtration [65,66]. Note that the steady-state flux was still reached despite the very low shear wall stress in this study (i.e. $\tau_w << 10$ Pa) (Fig. 4).

At both studied temperatures, rinsing–relaxation resulted in a roughly 90% decrease in fouling, although the average residual fouling resistance after this step was still significantly higher than the clean membrane resistance $R_r/R_m \approx$ 6–7 (Fig. 5). However, this conclusion is not universal: according to previous studies, an increase in temperature can increase [20,21,56], decrease [56,67] or not significantly influence [12,56] membrane fouling during skim milk filtration. It has also been reported that the temperature increase in the range of approximately 10–50 °C can decrease [12,21], increase [20] or not significantly influence [67] fouling removal efficiency (i.e. average residual membrane fouling). Note that different milk preparation protocols (storage, thermal treatment, cooling, powder rehydration, etc.) can influence filtration and account for these inconsistent results. Furthermore, as stated in the introduction, the lack of common results may reflect the complexity of filtration and fouling removal processes, and further argues against drawing general conclusions concerning optimal filtration conditions and fouling layer properties based on comparison of averaged filtration data (average flux or fouled membrane resistance). Therefore, an additional analysis of local fouling behavior was applied below in order to determine the influence of temperature on fouling layer formation and removal.

3.2. Fouling layer development during filtration

Fig. 6 presents *in situ* SAXS data on casein micelle accumulation in the concentration polarization layer during filtration at a constant applied pressure.

At both studied temperatures, a distinct concentration polarization layer was obtained on the membrane surface. The evolution of concentration profiles $c(z)$ over the course of filtration was similar to that obtained in Ref. [49] during crossflow filtration of skim milk at 25 °C:

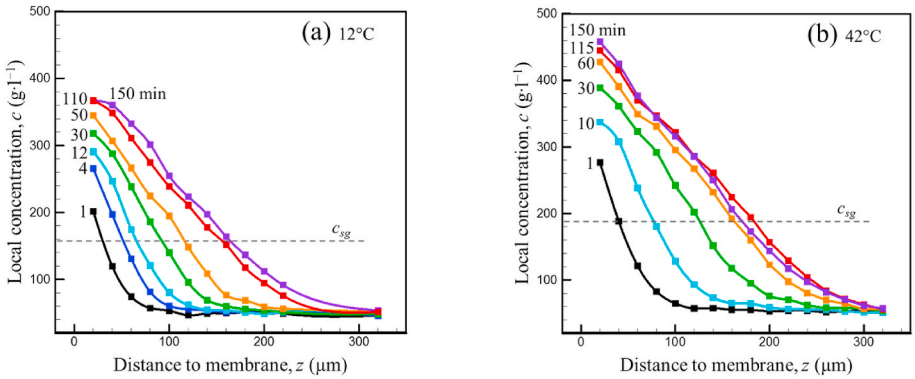

Fig. 6. Local casein concentration plotted against distance to membrane during crossflow filtration at 12 °C (a) and 42 °C (b) measured via SAXS. TMP = 110 kPa, v = 3.1 cm s^{-1}, filtration time t_F (in min) is shown near the curves. Dashed lines show the sol–gel transition concentration c_{sg} evaluated via Eq. (3).

casein concentration gradually increased as it neared the membrane surface, and the concentration polarization layer got thicker and more concentrated with filtration time. Therefore, the excess weight accumulated in the fouling layer m_{ex} (estimated via Eq. (1) and presented in Fig. 7a). constantly increased during filtration.

Casein micelle accumulation in the fouling layer was faster at 42 °C than at 12 °C, likely due to a higher flux of micelles to the membrane (Fig. 4). Interestingly, the m_{ex} value (which is the measure of local external membrane fouling) did not reach the plateau at t_F = 50 min (Fig. 7a) whereas filtrate flux reached a constant value at T = 12 °C and 42 °C (Fig. 4). This can be explained by a higher sensitivity of local concentration measurement compared to average flux measurement. In any case, it highlights that the average flux and fouling resistance analysis are not sufficient to characterize the kinetics of local membrane fouling, which was more severe at higher x. Nevertheless, at the end of the filtration step, the locally reached value of m_{ex} and local membrane fouling was higher at 42 °C than at 12 °C (Fig. 7a), which is consistent with the higher average fouled membrane resistance value (Fig. 4).

3.3. Fouling layer at the steady-state

After 150 min of filtration, when the build-up of the fouling layer slowed down significantly (Fig. 7a), the concentrated polarization was far stronger at 42 °C than at 12 °C (Fig. 6) even though the same TMP of 110 kPa had been applied. Total membrane fouling (i.e. average over the membrane length) and local external membrane fouling were significant at both temperatures (Figs. 5 and 6): i.e. the hydraulic resistance of the membrane covered with the deposit was significantly higher than the hydraulic resistance of clean membrane. It is therefore reasonable to assume that TMP was mainly exerted on the concentration polarization layer and not on the membrane [68]. We can consequently expect to find

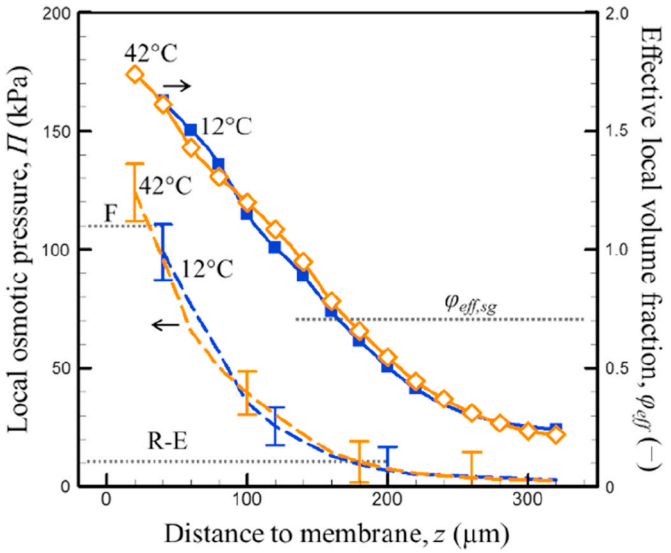

Fig. 8. Effective volume fraction of casein micelles in the fouling layer ϕ_{eff} versus distance to the membrane surface at the end of the filtration step at 12 °C (filled symbols) and 42 °C (open symbols) (TMP = 110 kPa, t_F = 150 min). Dashed curves represent the local osmotic pressure distribution $\Pi(z)$ calculated from $\phi_{eff}(z)$ and $\Pi(\phi_{eff})$ [41], error bars represent the 95% confidence interval for values $\Pi(\phi_{eff})$ obtained with fitting equation (S3). Dotted horizontals represent the expected sol–gel transition concentration $\phi_{eff,sg}$ [41] and the TMP values applied during the filtration (F) and pressure relaxation–erosion (R–E) steps.

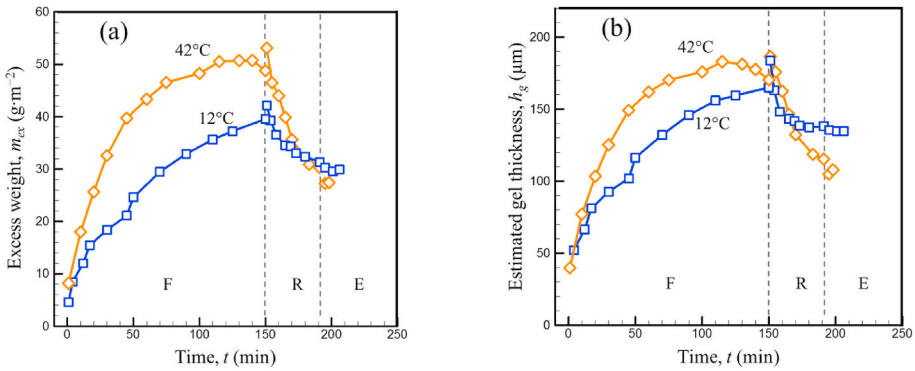

Fig. 7. Excess weight accumulated in the fouling layer m_{ex} (a) and estimated gel thickness h_g (b) plotted against time during the filtration (F), pressure relaxation (R) and erosion (E) steps of the experiment at 12 °C and 42 °C. Experimental conditions are given in Fig. 2.

similar layer compression at 12 °C and at 42 °C: i.e. the compressive pressure applied to the fouling layer was practically equal to the value of TMP and was therefore the same at 12 °C as at 42 °C. Working up from this conclusion, the observed difference in final $c(z)$ (Fig. 6) can be related to the difference in compressibility of casein micelles. According to Ref. [41] who studied casein micelles at 7 °C and 20 °C, the osmotic pressure of casein micelle dispersions Π increased with decreasing temperature for a given casein micelle concentration c. However, Π was equal at both temperatures at the same effective casein micelle volume fraction ϕ_{eff} (see Supplementary material). Fig. 8 charts the ϕ_{eff} (z) profiles obtained via Eq. (3) from the final $c(z)$ profiles at 12 °C and 42 °C.

In contrast to $c(z)$, the $\phi_{eff}(z)$ profiles overlapped closely at 12 °C and 42 °C. Obtained values of ϕ_{eff} were used for evaluation of local osmotic pressure distribution in deposits $\Pi(z)$ (Fig. 8 dashed curves). $\Pi(z)$ were evaluated with using the $\Pi(\phi_{eff})$ relation previously reported for casein micelle dispersions at 7°C-20 °C (Supplementary material). It must be noted that somewhat overestimated values of osmotic pressure were obtained, because Π in the deposit during filtration cannot exceed TMP. This can be explained by the complex method used for osmotic pressure evaluation, which gives a noticeable error (error bars in Fig. 8). Nevertheless, evaluated dependency of osmotic pressure on distance to membrane $\Pi(z)$ was practically the same at both temperatures. This suggests that the higher fouling layer concentration c observed at 42 °C (Fig. 6) can be explained by temperature-enhanced compression (i.e. shrinkage) of casein micelles. Increasing system compressibility (at 42 °C) thus equates to increasing concentration level in the deposit, at the same external TMP. Note that the values $\phi_{eff} > 1$ were obtained for the inner part of the fouling layer, which signals that casein micelles themselves were compressed and, probably, deformed near the membrane surface [43,69], where Π approached the value of TMP = 110 kPa.

3.4. Fouling layer behavior during pressure relaxation and erosion steps

According to Fig. 6, the casein micelle concentration in the vicinity of the membrane surface exceeded the sol–gel transition concentration (c_{sg} = 157 g l^{-1} at 12 °C and 189 g l^{-1} at 42 °C) from the beginning of filtration. Gel thickness progressively increased during filtration (Fig. 7b) to ultimately result in severe membrane fouling with $h_g \approx 170$ μm at t_F = 150 min (Fig. 8). Subsequently, TMP was decreased (relaxation) and average crossflow velocity was increased (erosion) in order to study the 'strength' of the fouling (Fig. 2).

3.4.1. Amount of casein micelles in the concentration polarization layer m_{ex} and gel thickness h_g

Note that m_{ex} and h_g increased abruptly when the filtration pressure relaxed (Fig. 7). This can be explained by an instant shift of the flexible polymeric filtration membrane away from the rigid membrane support due to the instant reduction of TMP [70,71] (although a low TMP of 10 kPa was maintained in order to reduce this effect during the pressure relaxation). The shift of the membrane towards positive z brought the inner sublayer of casein micelles, which was localized close to the membrane surface ($z < 20$ μm) and was not accounted for in the calculations of m_{ex} and h_g during the earlier filtration step, into the scope of SAXS analysis ($z > 20$ μm) [70,71], resulting in an apparent increase of m_{ex} and h_g. According to Fig. 7b, the membrane shifted for 16–17 μm, which was small compared to the lowest measured gel thickness at the end of erosion step (h_g = 108 μm at 12 °C).

Both m_{ex} and especially h_g gradually decreased during the relaxation and erosion steps (Fig. 7). This gradual evolution of the local fouling layer was consistent with previous studies of membrane cleaning and rinsing after skim milk ultrafiltration [8,11,16,32,33] where membrane fouling removal by rinsing and pressure relaxation (evaluated from the average membrane resistance or the total quantity of removed foulant) was found to be a continuous process. However, in contrast to previous studies where crossflow significantly accelerated fouling removal [8,11,16,32,33], in the current study the five-fold increase in crossflow velocity had no net impact on $m_{ex}(t)$ and $h_g(t)$, especially at 12 °C (Fig. 7).

3.4.2. Local concentration distribution in the fouling layer

In order to clarify the fouling removal mechanism (and explain the discrepancy with observations made in Ref. [8,11,16,32,33]), we analyzed local concentration distribution in the fouling layer during the relaxation and erosion steps (Fig. 9).

At both studied temperatures, local casein concentration decreased at any distance from the membrane surface (Fig. 9), indicating removal and swelling of the casein micelle deposit during the relaxation and erosion steps. Based on these results (Fig. 9), one could differentiate two relaxation behaviors of the fouling layers at different distances from the membrane. These two different behaviors allowed us to define what we call the 'inner part' of the gel near the membrane surface (from z = 20 μm–100 μm) where casein micelle concentration did not vary a lot with time, and the 'outer part' of the layer farther away from the membrane surface (from z = 100 μm to > 300 μm), where casein concentration profile decreased sharply with time.

Notably, a slight decrease of $c(t)$ was observed in the inner part of the gelled fraction of the fouling layer (Fig. 9), even though it was not in direct contact with crossflowing bulk suspension, which rules out direct gel erosion. Therefore, it can be assumed that the decrease in local concentration in the gel was due to gel swelling driven by the osmotic pressure gradient [72], which seemed to exist between the compressed gel and the bulk dispersion (Fig. 8). As expected for a diffusion-type process, the gel swelling slowed gradually with time (i.e. with the decrease of gel concentration and osmotic pressure).

In addition, the increase of crossflow velocity at the erosion step had an immediate effect on the outer part of the fouling layer (sol) but practically no effect on its inner gelled part. This suggests that the low shear stress applied (maximal value $\tau_w \approx 1$ Pa during erosion at 12 °C) was not high enough to detach micelles from the non-swelled gel surface and was only effective in removing the liquid component of concentration polarization.

The foulant casein micelle gel cannot, therefore, be defined as completely irreversible, as it swelled and re-dispersed at both studied temperatures. However, the following observations highlight the need for in-depth analysis of the gel swelling in order to make firm conclusions on the reversibility of membrane fouling.

First, fouling removal was slower at 12 °C than 42 °C (Fig. 7), but at the same time, the evaluated initial osmotic pressure gradients across the gel and gel thickness were the same at 12 °C and 42 °C (as discussed in the analysis of Fig. 9). It is therefore necessary to verify whether the difference in fouling removal can be fully explained by higher liquid viscosity and, therefore, slower liquid diffusion into the gel at lower temperature.

Second, a slowdown of the local concentration decrease was more notable for the inner part of the gel layer ($z < 100$ μm, $t_R >$ 8–10 min in Fig. 9), even though this part was effectively more compressed during filtration compared to the outer part of the concentration polarization layer (where the concentration continued to decrease).

In-depth analysis of the gel swelling process is thus required.

3.4.3. Analysis of gel swelling

In order to analyze the behavior of the fouling layer at different temperatures and degrees of compression, we compared the swelling kinetics at 12 °C and 42 °C in gel 'sub-layers' having the same initial local effective casein micelle volume fractions (Fig. 10) and consequently the same values of end-of-filtration compressive osmotic pressure (Fig. 8). Fig. 10 reports the ϕ_{eff} values as a function of $t \cdot \mu^{-1}$ in order to exclude from analysis the evident effect of temperature dependence of viscosity on liquid uptake during the swelling (which slows down swelling at 12 °C compared to 42 °C).

The swelling kinetics (Fig. 10) emerge properties of compressed casein micelle layers:

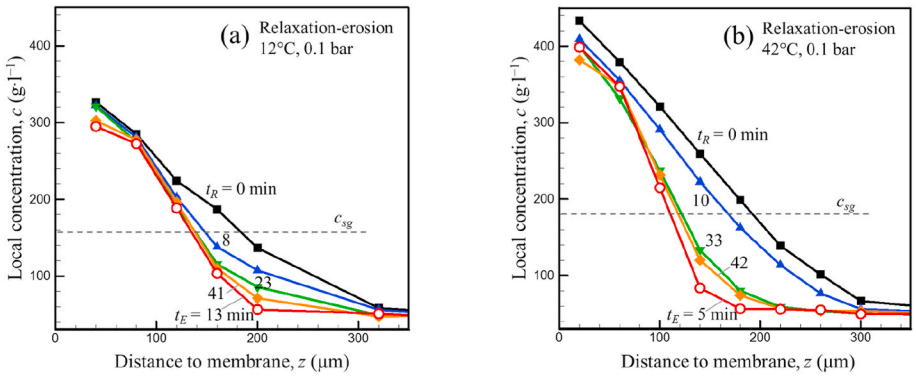

Fig. 9. Local casein concentration versus distance to membrane during the pressure relaxation (filled symbols) and erosion (open symbols) steps at 12 °C (a) and 42 °C (b). Time from the beginning of each step is shown near the curves (in min). Dashed horizontals show the estimated sol–gel transition concentration, t_R – relaxation time, t_E – erosion time.

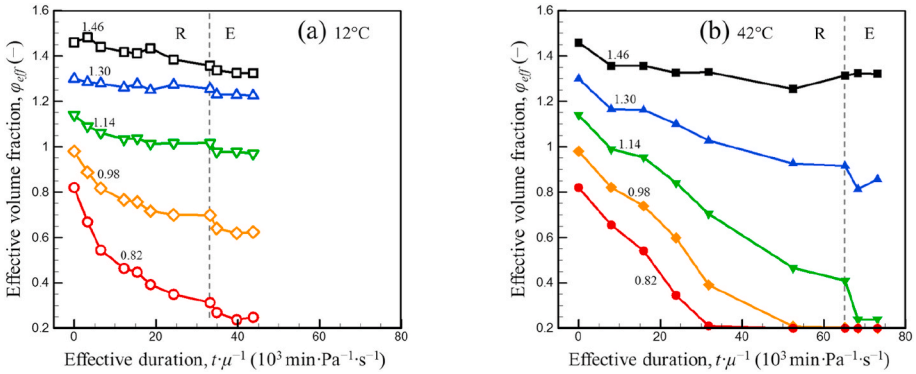

Fig. 10. Evolution of the effective volume fraction of casein micelles within the gel layer during pressure relaxation (R) and subsequent erosion (E) at 12 °C and 42 °C. The dashed vertical indicates the point of crossflow velocity increase from $v = 3.1$ cm s^{-1} (relaxation) to 15.6 cm s^{-1} (erosion). Initial (at the beginning of relaxation) values of ϕ_{eff} within the studied 'sub-layers' are shown near the curves.

(1) At both studied temperatures, initial swelling rate ($d\phi_{eff}/dt$) decreased with increasing local initial layer concentration ϕ_{eff} (i.e. as the layer approached the membrane surface). Meanwhile, according to modelling in Ref. [72], in the case of completely reversible compression of casein micelle deposits, the swelling is faster in the more compressed inner part of the gel (i.e. closer to the membrane surface) than in its less compressed outer part. According to filtration–consolidation theory, the initial swelling rate is mainly determined by initial (osmotic) pressure gradient-driven swelling [72], which is equal to compressive pressure in the case of completely reversible compression. Therefore, based on the qualitative discrepancy between the experimental and modelled results on the local swelling rate of the casein micelle fouling gel layer (Fig. 10 and [72], respectively), it can be concluded that the compression of casein micelles was not completely reversible: swelling was slower than expected for a fully reversibly compressible gel and this discrepancy increased with the increasing of initial degree of compression.

(2) At the highest studied degree of compression (e.g. $\phi_{eff} = 1.46$ in Fig. 10), the specific kinetics of swelling (ϕ_{eff} versus $t_R \cdot \mu^{-1}$) was practically temperature-independent; however, the swelling remained very limited, as it plateaued at $\phi_{eff} \approx 1.33$. Furthermore, when the initial degree of compression decreased from 1.46 to 0.82 (i.e. practically to the sol–gel transition concentration according to Ref. [41], $\phi_{sg} = 0.71$), the swelling was notably faster at 42 °C compared to 12 °C. In addition to this difference, ϕ_{eff} tended to reach constant levels (that decreased with decreasing of initial degree of compression) at 12 °C whereas there were no visible plateaus at 42 °C (though lower ϕ_{eff} were reached during swelling before the erosion step at 42 °C than at 12 °C). This may mean that gel compression was less reversible at 12 °C than at 42 °C. The difference in swelling kinetics at 12 °C vs. 42 °C decreased with decreasing initial ϕ_{eff} and practically vanished at low initial degree of compression $\phi_{eff} \leq 0.82$. This observation also suggested that the irreversibility of compression increased with increasing degree of initial compression (especially at 12 °C where there was limited swelling of the compressed layer).

(3) Increasing crossflow velocity at the erosion step of the experiment only influenced gel layers that had sufficiently swelled. At both temperatures, the erosion step had practically no effect on the layer with initial $\phi_{eff} \geq 1.30$. At 42 °C, the increase of the crossflow velocity removed the part of the gel that swelled from the initial concentration $\phi_{eff} \leq 1.22$ to $\phi_{eff} \leq 0.6$ (i.e. below the sol–gel transition concentration $\phi_{sg} = 0.71$) (data not shown). However, at 12 °C the outer gel layer was replaced by bulk suspension only after swelling from $\phi_{eff} = 0.86$ to 0.37, i.e. to a concentration that was significantly lower than ϕ_{sg} (data not shown). It can be concluded that at 12 °C, the swelling below the sol–gel transition concentration did not lead to gel dissociation, as dissociation required further swelling to $\phi_{eff} < \phi_{sg}$. In other words, at 12 °C, $\phi_{gs} < \phi_{sg}$, and ϕ_{gs} was only reached at low levels of initial gel compression.

Note that this local analysis of relaxation of the gelled fouling layer obtained by crossflow filtration of casein micelle dispersions confirms and supports the central conclusions of [40] drawn from observation of

swelling-redispersion in gels prepared from casein micelle dispersions by osmotic compression at 20 °C: (i) the reversibility of compression strongly decreases with initial gel deformation (i.e. the gel concentration reached during osmotic compression); during the swelling, the gel can keep its cohesiveness (i.e. does not disperse spontaneously, without agitation) while reaching the volume fraction that is lower than the sol–gel formation concentration ϕ_{sg} [40]. Explained this partial reversibility (the gel swells but remains solid at $\phi < \phi_{sg}$) by the formation of cohesive bonds between the compressed micelles. According to Ref. [40], there is a minimal critical level of compression required for partial irreversibility to appear, and it corresponds to the concentration marking the mechanical collapse of the steric barrier created by the κ-casein "brush". If this explanation of irreversibility is true, then our findings confirm that cohesive bonds can appear in a shorter filtration experiment timeframe than in Ref. [40] where the samples were compressed for several weeks before the relaxation. This conclusion is also supported by a recent study in which the appearance of cohesion between casein micelles and covered fat droplets was explicitly detected via AFM after 1 s of probe-to-substrate contact [73]. This also implies that the cohesiveness of the swelling gel increases at lower studied temperature (12 °C).

The current data also explicitly confirms the result of [37], where the appearance of a cohesive but swelling gel of casein micelles on the ultrafiltration membrane surface was indirectly studied via analysis of fouled membrane resistance after membrane rinsing with pressure relaxation after filtration at minimal critical TMP. The results presented in Figs. 8 and 10 suggest that the minimal critical TMP required for the partially irreversible (i.e. swelling but cohesive) gel formation must increase with the temperature increase from 12 °C to 42 °C.

3.5. Average data versus local data on fouling removal

The swelling analysis performed in the previous section suggested that the fouling removal mechanism was gel swelling and redispersion of a sufficiently swelled part of the gel layer into the bulk (together with the initially liquid part of the concentration polarization layer). Note that deposit swelling or diffusion (and, therefore, pressure relaxation) was reported to play an important role in the removal of external membrane fouling after skim milk filtration in Ref. [8], where average residual membrane fouling after rinsing–relaxation was accessed by measuring flux and concentration of foulant in the rinsing liquid. In this regard, it is interesting to highlight the difference, which was observed in the current study between the results of conventional average (Fig. 5) and proposed local (Fig. 7) fouling analysis. According to the average analysis (Fig. 5, with values averaged over the membrane length $L = 10$ cm), the rinsing–relaxation step reduced membrane fouling by 90% without any notable influence of temperature on fouling removal. However, our local fouling analysis (Fig. 7, values obtained for the center of the filter channel, $x = 5$ cm) revealed substantially less foulant removal, i.e. 20 % at 12 °C and 40% at 42 °C. The difference between the average and local data can be explained by the expected distribution of fouling layer thickness and concentration along the membrane length: gel thickness h_g decreases with decreasing x [36], and rate of swelling, which is a diffusion-like process, must decrease inversely to h_g^2 [72,74]. Therefore, gel swelling and subsequent removal were significantly faster at $x < 5$ cm whereas the average flux value measured after rinsing–relaxation was more sensitive to the higher local flux at $x < 5$ cm. Here again, local data analysis proves crucial to fully characterize membrane fouling.

3.6. Discussion on related literature data and filtration practice

With the exclusion of a handful of papers discussed above, there is too little published data available on membrane fouling by casein micelle dispersions for direct comparison with our current results [11]. Reported that the fouling layer obtained during dead-end filtration of casein micelle dispersions can be removed by continuous pressure relaxation with slow crossflow ($t_R \approx 1000$ min, $\tau_w \approx 1$ mPa) despite a high TMP applied during filtration (up to 400 kPa). This result is different from our conclusion on limited swelling and redispersion of gel layers obtained at high compressive pressure (Fig. 10). However, the results of [11] may signify that the cohesiveness of casein micelles decreases with time and disappears at $t_R \approx 1000$ min. The same idea was previously proposed to explain spontaneous redispersion of concentrated casein micelles gels at $t_R \approx 200$ h [40,42], and it also agrees well with the theory and with numerous experimental data on the time and velocity dependency of adhesion between two surfaces covered with polymer brushes (e.g. Ref. [75]), which is a good proxy for neighboring casein micelles in swelling deposits. That aid, based on data presented in Fig. 10, filtration practice should aim to avoid highly compressed gels of casein micelles as they show limited swelling and redispersion.

A majority of studies on the reversibility of membrane fouling have been carried out with skim milk. Note that there is no single consensus on the role of casein micelles in membrane fouling during the milk filtration, which is reported as major [25,31,32] or insignificant [21,35], without confirmed explanation for this difference (although possible reasons are discussed in the Introduction and Appendix). Nevertheless, our conclusion that higher compressive pressures forms more cohesive and less swellable gel is consistent with numerous data on the skim milk filtration: increasing filtration pressure results in slower recovery of membrane resistance during subsequent rinsing and pressure relaxation and higher residual membrane fouling at $T = 14$ °C [32], 40 °C [33] and 48–50 °C [7,17,30]. The results [32,33] and [7,17,30] were obtained via conventional analysis of average membrane resistance, without directly observing gel formation on the membrane surface.

In contrast, Piry et al. [10] studied reversibility of membrane fouling by deposit during microfiltration of skim milk at 55 °C in original filter cell that allowed measuring of local hydraulic resistance of fouled membrane at known local TMP before and after the rinsing. It was observed that rinsing allowed to reduce the fouling resistance significantly; therefore, it allowed to remove the largest part of deposit obtained at TMP ≥45–110 kPa [10] (unfortunately, conditions of rinsing as well as the deposit removal mechanism were not detailed). Moreover, it was observed that higher local membrane fouling by deposit (that was obtained at higher local TMP) also resulted in higher residual membrane fouling resistance. Although local fouling resistances were compared at different local TMP (that complicates the data analysis in the studied case of compressible deposit, because higher residual resistance may correspond to higher deposit compression and not to higher residual deposit thickness), it can be assumed that these results of [10] for skim milk deposit are also compatible with our conclusion about negative impact of locally attained compression on reversibility of casein micelle deposit.

Also [29], applied *in situ* MRI to study of skim milk filtration at 25 °C and demonstrated that the external membrane fouling layer can be completely removed by diffusion when it is obtained by filtration at 50 kPa but remains on the surface if initial filtration pressure is 150 kPa. This direct observation is in qualitative agreement with our conclusions on the role of filtration pressure in the reversibility of compression of casein micelle deposition.

The influence of temperature on fouling layer structure and properties is studied very rarely, only data for skim milk filtration are available. For example [79], concluded from *in situ* MRI analysis of dead-end filtration of skim milk that deposit obtained at 45 °C (and mostly composed of casein micelles) is denser (i.e. more concentrated) than that obtained at 22 °C. This is in accordance with data presented in Fig. 6.

In contrast, data equivalent to that in Fig. 5 are abundant for skim milk filtration. According to our data (obtained for 12 °C and 42 °C for casein micelle dispersions), stronger membrane fouling was obtained at lower filtration temperature. This is in qualitative agreement with [20,

33]: lower temperature results in stronger membrane fouling (when comparing 10 °C vs. 50 °C for pasteurized skim milk). However [12,21], arrived at different conclusion (also when comparing 10 °C vs. 50 °C for pasteurized skim milk).

Hartinger et al. [12] compared reversibility of membrane fouling by deposit during skim milk filtration in a spiral-wound module at 10 °C and 50 °C. The average hydraulic resistance of fouled membrane R_f was measured at a constant cross-flow velocity during stepwise increase of the average TMP to 300 kPa and its following stepwise decrease to 50 kPa (with constant step duration). At both studied temperatures, limiting flux was attained at TMP ≈150 kPa, that allowed the authors to relate the following variation of R_f with a response of deposit on the variation of TMP (i.e. their averages). At 10 °C the steady-state value of R_f was obtained at each step of experiment, and dependencies of R_f on TMP matched during the pressure increase and pressure decrease. This was explained by complete reversibility of deposit obtained at 10 °C (however, neither deposit removal mechanism nor the role of deposit decompression and particles redispersion were detailed). In contrast, at 50 °C steady-state was not attained during the pressure increase phase of experiment. This was explained by deposit aging due to the temperature induced proteins interaction inside the deposit. The values of R_f obtained during the TMP decrease were higher as compared to those obtained during the TMP increase. This difference was explained by (at least partial) irreversibility of deposit obtained at 50 °C that consisted of interconnected compressed proteins (though it is unclear, if this difference disappears if the steady-state is reached and higher values of R_f are obtained during the deposit formation). Interesting that deposit compression resulted in irreversible (at least partially) decrease of transmission of serum proteins (even at 10 °C, when R_f was restored after the pressure decrease). Therefore, it was concluded that during milk filtration transmission of serum proteins is not directly related with deposit resistance [12].

It can be seen that direct comparison of our data on local structure of deposit obtained during casein micelles filtration at 12 °C and 42 °C at rather low shear stress with data of [12] on the hysteresis of average *Rf* (TMP) obtained during the skim milk filtration at 10 °C and 50 °C at certainly higher shear stress is difficult. Nevertheless, our conclusions about the influence of temperature of deposit reversibility are opposite to those of [12]. We assume that this divergence can be explained by the difference in composition of filtered fluids, i.e. by role of serum proteins in casein micelles interaction. It is possible that temperature-induced aggregation of β-lactoglobulin is responsible for casein micelles "gluing" in the deposit obtained at 50 °C in Ref. [12], while at 10 °C presence of β-lactoglobulin increases steric barrier between the micelles (that would otherwise interact). This idea can be verified in a future by comparison of filtration of casein micelle dispersion and skim milk (or mixed protein dispersions) at low and high temperatures (carried out either as in our current study or as in Ref. [12]).

Too little is published on the deposit swelling kinetics: though swelling of casein micelle deposits obtained at different TMP was previously studied by Qu et al. [37], the swelling kinetics was not characterized in their paper. However, Weinberger and Kulozik [80] studied variation of deposit properties (assessed from unsteady values of average fouled membrane resistance obtained in the limiting flux conditions) during microfiltration of skim milk at 15 °C with rapid cyclic variation of average TMP and cross-flow velocity (pulsatile flow). It was observed that R_f decreased in several times in less than 5 s, when the TMP decreased from 180 kPa to 10 kPa (approximately). The authors assumed that rapid decrease of R_f was due the deposit swelling (i.e., the deposit compression was reversible). Though local deposit quantity is not directly proportional to R_f (because R_f is also defined by TMP), it can be noted that [80] reported very fast swelling in contrast to our present study (seconds [80] versus tens of minutes, Fig. 7). This large difference can be explained by significantly lower membrane fouling: in Ref. [80] R_f was of the order of 10^{12} m^{-1}, while in our study $R_f \approx 5\times10^{14}$ at TMP = 110 kPa (Fig. 5). As soon as R_f is proportional to h_g and the swelling time is proportional to h_g^2, the hundredfold difference in R_f should increase the swelling duration in 10^4 times. The cycle duration in Ref. [80] was too short to verify, if the swelling of deposit obtained at 15 °C can be followed by redispersion (i.e. if the deposit formation was reversible).

Also, it is possible that different papers are actually discussing different types of fouling (blocked pores, absorbed monolayer, gel), in which case there would be various reasons to explain the different temperature effects reported. In the present study casein micelle gelling play a driving role in the fouling mechanism, and so the negative impact of temperature decrease on gel reversibility (Fig. 10) is probably related to the temperature impact on casein micelle composition and voluminosity. For example, in contrast to the result presented in Fig. 7 , [8,13,32,34] observed very small residual foulant quantity corresponding to 1–2 monolayers of casein micelles (likely, due to the vigorous rinsing), which may be insensitive to the TMP of fouling layer formation. However, rigorous and uniform membrane rinsing is not always possible at industrial scale in spiral wound modules.

The importance of swelling for deposit erosion (Fig. 10) also suggests that external fouling could be more efficiently removed by not applying TMP when rinsing the membrane (this idea has already been voiced [77–79], also in the milk filtration literature [8]). This is because applied TMP counteracts the osmotic swelling pressure and reduces the swelling.

4. Conclusions

Crossflow ultrafiltration of casein micelle dispersions was studied at 12 °C and 42 °C by *in situ* SAXS, enabling us to time-resolved spatial information on the local concentration in the vicinity of the membrane surface at distances down to a few hundred micrometers with a resolution of 20 μm. Local solid concentration distribution and average filtrate flux were measured and analyzed at different experiment steps (filtration, pressure relaxation, erosion).

Filtrate flux was higher at 42 °C than at 12 °C, which could be partially explained by lower filtrate viscosity. Despite differences in thickness and local dry matter concentration (both were higher at 42 °C), the estimated local structure of the fouling layer (i.e. dependency of effective volume fraction of the casein micelles on local osmotic pressure, $\phi_{eff}(\Pi)$) was not significantly influenced by filtration temperature. Casein micelles were compressed ($\phi_{eff} > 1$) in the inner part of the deposit.

At both temperatures studied, pressure relaxation resulted in deposit swelling (including its inner part with $\phi_{eff} > 1$) and continuous removal of the outer swelled part of the fouling layer. Analysis of local concentration profiles suggested that swelling was less rapid than expected in the inner, more compressed part of the deposit that can be explained by the partial irreversibility of the deposit compression. Moreover, swelling was found to be slower at 12 °C than at 42 °C. Slower swelling reduced fouling layer removability.

Quantitative characterization of fouling reversibility requires more elaborate analysis of local swelling data, which will be done in our following study. Note that the fouling removal mechanism must depend on the filtration and rinsing conditions (therefore, role of swelling on fouling removal can vary with increasing of the wall shear stress applied during the rinsing, that should be studied in a future) as well as on serum composition (i.e. presence of soluble proteins). Therefore, gel–membrane interactions and the properties of deposits obtained during skim milk filtration require further in-depth study. The results reported here (together with literature analysis) underline that local data analysis is essential for in-depth characterization of membrane fouling.

Author Statement

Each co-author made equally important input to this article

Declaration of competing interest

The authors declare that they have no known competing financial interests or personal relationships that could have appeared to influence the work reported in this paper.

Acknowledgments

We thank the French National Research Institute for Agriculture, Food and Environment (INRAE) and the Brittany Regional Council for providing valuable financial support. We also thank the SOLEIL Synchrotron for providing synchrotron beam time and further financial support (project ID: 2017023). We thank Glen McCulley for invaluable help preparing the manuscript.

LRP is part of PolyNat Carnot Institute ('Investissements d'Avenir'–grant agreement #ANR-11-CARN-030-01), Labex TEC 21 ('Investissements d'Avenir'–grant agreement #ANR-11-LABX-0030) and Glyco@Alps ('Investissements d'Avenir'–grant agreement #ANR-15-IDEX-02).

Appendix A. Supplementary data

Supplementary data to this article can be found online at https://doi.org/10.1016/j.memsci.2020.118700.

Appendix. On the analysis of membrane fouling in the milk filtration literature

Analysis and comparison of published data on membrane fouling in milk filtration is made difficult by a number of reasons, as set out below.

1. Most of the reported data on milk filtration comes from case studies where the membrane is fouled at a single combination of transmembrane pressure and average crossflow velocity. However, fouling mechanism and intensity vary with filtration process parameters (e.g. transmembrane pressure and wall shear stress) and depend on filter cell geometry (e.g. use of spacers, filter channel length). This makes it a challenge to determine the fouling regime (e.g. to determine whether filtration was limited by deposit formation or adsorption) based on the limited information available concerning key filtration parameters. It also devalues subsequent analysis of fouling removal (as it concerns an undefined type of fouling).
2. The characterization of fouling removal often lacks precision. Like fouling formation, fouling removal can prove a complex and continuous process in milk filtration, which generally involves various possible fouling removal mechanisms. The intensity of fouling that remains at the membrane (which is questionably called 'irreversible fouling') may depend on cleaning-operation conditions (e.g. transmembrane pressure, crossflow velocity, turbulence, duration of the rinsing cycle). Despite this, a number of papers discuss 'irreversible' fouling after 'simple' (and, therefore, undetailed) membrane rinsing.
3. In the vast majority of articles, the intensity of fouling is characterized by so-called 'reversible' and 'irreversible' membrane fouling resistances, which are obtained by measuring water flux though a fouled and cleaned membrane. Although these parameters are technically important, it should be noted that they represent an average intensity of fouling, whereas fouling intensity can be non-homogeneously distributed over the membrane surface. Therefore, average parameters do not characterize the fouling (especially, hydraulic resistance) sufficiently well.
4. Fouling mechanism (pore blocking, adsorption, deposit adhesion) can vary with membrane type and material, and with membrane treatment history.

References

[1] G. Gésan-Guiziou, Separation technologies in dairy and egg processing, in: S.S. H. Rizvi (Ed.), Separation, Extraction and Concentration Processes in the Food, Beverage and Nutraceutical Industries, Woodhead Publishing Ltd., 2010, pp. 341–380.
[2] K.S.Y. Ng, M. Haribabu, D.J.E. Harvie, D.E. Dunstan, G.J.O. Martin, Mechanisms of flux decline in skim milk ultrafiltration: a review, J. Membr. Sci. 523 (2017) 144–162.
[3] M. Rabiller-Baudry, M. Le Maux, B. Chaufer, L. Begoin, Characterisation of cleaned and fouled membrane by ATR-FTIR and EDX analysis coupled with SEM: application to UF of skimmed milk with a PES membrane, Desalination 146 (2002) 123–128.
[4] M. Rabiller-Baudry, L. Paugam, L. Begoin, D. Delaunay, M. Fernandez-Cruz, C. Phina-Ziebin, C. Laviades-Garcia de Guadiana, B. Chaufer, Alkaline cleaning of PES membranes used in skimmed milk ultrafiltration: from reactor to spiral-wound module via a plate-and-frame module, Desalination 191 (2006) 334–343.
[5] G. Gésan-Guiziou, A.P. Sobantka, S. Omont, D. Froelich, M. Rabiller-Baudry, F. Thueux, D. Beudon, L. Trégret, C. Buson, D. Auffret, Life Cycle Assessment of a milk protein fractionation process: contribution of the production and the cleaning stages at unit process level, Separ. Purif. Technol. 224 (2019) 591–610.
[6] O. Le Berre, G. Daufin, Skimmilk crossflow microfiltration performance versus permeation flux to wall shear stress ratio, J. Membr. Sci. 117 (1996) 261–270.
[7] G. Gésan-Guiziou, E. Boyaval, G. Daufin, Critical stability conditions in crossflow microfiltration of skimmed milk: transition to irreversible deposition, J. Membr. Sci. 158 (1999) 211–222.
[8] K. Nakanishi, H.-G. Kessler, Rinsing behavior of deposited layers formed on membranes in ultrafiltration, J. Food Sci. 50 (1985) 1726–1731.
[9] W. Kuhnl, A. Piry, V. Kaufmann, T. Grein, S. Ripperger, U. Kulozik, Impact of colloidal interactions on the flux in cross-flow microfiltration of milk at different pH values: a surface energy approach, J. Membr. Sci. 352 (2010) 107–115.
[10] A. Piry, A. Heino, W. Kuhnl, T. Grein, S. Ripperger, U. Kulozik, Effect of membrane length, membrane resistance, and filtration conditions on the fractionation of milk proteins by microfiltration, J. Dairy Sci. 95 (2012) 1590–1602.
[11] T. Steinhauer, J. Lonfat, I. Hager, R. Gebhardt, U. Kulozik, Effect of pH, transmembrane pressure and whey proteins on the properties of casein micelle deposit layers, J. Membr. Sci. 493 (2015) 452–459.
[12] M. Hartinger, H.-J. Heidebrecht, S. Schiffer, J. Dumpler, U. Kulozik, Milk protein fractionation by means of spiral-wound microfiltration membranes: effect of the pressure adjustment mode and temperature on flux and protein permeation, Foods 8 (2019), 8060180.
[13] N. Wemsy Diagne, M. Rabiller-Baudry, L. Paugam, On the actual cleanability of polyethersulfone membrane fouled by proteins at critical or limiting flux, J. Membr. Sci. 425–426 (2013) 40–47.
[14] H. Bouzid, M. Rabiller-Baudry, L. Paugam, F. Rousseau, Z. Derriche, N.E. Bettahar, Impact of zeta potential and size of caseins as precursors of fouling deposit on limiting and critical fluxes in spiral ultrafiltration of modified skim milks, J. Membr. Sci. 314 (2008) 67–75.
[15] D. Delaunay, M. Rabiller-Baudry, J.M. Gozálvez-Zafrilla, B. Balannec, M. Frappart, L. Paugam, Mapping of protein fouling by FTIR-ATR as experimental tool to study membrane fouling and fluid velocity profile in various geometries and validation by CFD simulation, Chem. Eng. Process 47 (2008) 1106–1117.
[16] W. Zhang, L. Ding, M.Y. Jaffrin, B. Tang, Membrane cleaning assisted by high shear stress for restoring ultrafiltration membranes fouled by dairy wastewater, Chem. Eng. J. 325 (2017) 457–465.
[17] A.S. Grandison, W. Youravong, M.J. Lewis, Hydrodynamic factors affecting flux and fouling during ultrafiltration of skimmed milk, Lait 80 (2000) 165–174.
[18] W. Youravong, M.J. Lewis, A.S. Grandison, Critical flux in ultrafiltration of skimmed milk, Food Bioprod. Process. 81 (2003) 303–308.
[19] X. Luo, L. Ramchandran, T. Vasiljevic, Lower ultrafiltration temperature improves membrane performance and emulsifying properties of milk protein concentrates, Dairy Sci. Technol. 95 (2015) 15–31.
[20] S. Methot-Hains, S. Benoit, C. Bouchard, A. Doyen, L. Bazinet, Y. Pouliot, Effect of transmembrane pressure control on energy efficiency during skim milk concentration by ultrafiltration at 10 and 50°C, J. Dairy Sci. 99 (2016) 8655–8664.
[21] K.S.Y. Ng, D.E. Dunstan, G.J.O. Martin, Influence of processing temperature on flux decline during skim milk ultrafiltration, Separ. Purif. Technol. 195 (2018) 322–331.
[22] D. Tremblay-Marchand, A. Doyen, M. Britten, Y. Pouliot, A process efficiency assessment of serum protein removal from milk using ceramic graded permeability microfiltration membrane, J. Dairy Sci. 99 (2016) 5230–5243.
[23] C. Vetier, M. Bennasar, B.T. de la Fuente, Study of the fouling of a mineral microfiltration membrane using scanning electron microscopy and physicochemical analyses in the processing of milk, J. Dairy Res. 55 (1988) 381–400.
[24] M. Koutake, I. Matsuno, H. Nabetani, M. Nakajima, A. Watanabe, Osmotic pressure model of membrane fouling applied to the ultrafiltration of whey, J. Food Eng. 18 (1993) 313–334.
[25] T.J. Tan, D. Wang, C.I. Moraru, A physicochemical investigation of membrane fouling in cold microfiltration of skim milk, J. Dairy Sci. 97 (2014) 4759–4771.
[26] S. Popovic, M.N. Tekic, Twisted tapes as turbulence promoters in the microfiltration of milk, J. Membr. Sci. 384 (2011) 97–106.
[27] D.M. Krstic, M.N. Tekic, M.D. Caric, S.D. Milanovic, The effect of turbulence promoter on cross-flow microfiltration of skim milk, J. Membr. Sci. 208 (2002) 303–314.

[28] T. Mohammadi, S.S. Madaeni, M.K. Moghadam, Investigation of membrane fouling, Desalination 153 (2002) 155–160.
[29] N. Schork, S. Schuhmann, H. Nirschl, G. Guthausen, In situ measurement of deposit layer formation during skim milk filtration by MRI, Magn. Reson. Chem. 57 (2019) 738–748.
[30] G. Gésan-Guiziou, A. Jimenez, C. Arcelin, Cake properties in dead-end ultrafiltration of casein micelles: determination of critical operating conditions, Desalination 199 (2006) 20–22.
[31] A.J.E. Jimenez-Lopez, N. Leconte, O. Dehainault, C. Geneste, L. Fromont, G. Gésan-Guiziou, Role of milk constituents on critical conditions and deposit structure in skimmilk microfiltration (0.1 μm), Separ. Purif. Technol. 61 (2008) 33–43.
[32] H.G. Kessler, C. Gernedel, K. Nakanishi, The effect of low molecular weight milk constituents on the flux in ultrafiltration, Milchwissenschaft 37 (1982) 584–587.
[33] U. Kulozik, H.G. Kessler, Rinsing behaviour of deposited layers in reverse osmosis, Milchwissenschaft 43 (1988) 784–789.
[34] N.W. Diagne, M. Rabiller-Baudry, Cleanability versus limiting and critical fluxes of a polyethersulfone membrane of skim milk ultrafiltration, Procedia Engineer 44 (2012) 72–74.
[35] P.S. Tong, D.M. Barbano, W.K. Jordan, Characterization of proteinaceous membrane foulants from whey ultrafiltration, J. Dairy Sci. 72 (1988) 1435–1442.
[36] P. Bacchin, D. Si-Hassen, V. Starov, M.J. Clifton, P. Aimar, A unifying model for concentration polarization, gel-layer formation and particle deposition in cross-flow membrane filtration of colloidal suspensions, Chem. Eng. Sci. 57 (2002) 77–91.
[37] P. Qu, G. Gésan-Guiziou, A. Bouchoux, Dead-end filtration of sponge-like colloids: the case of casein micelle, J. Membr. Sci. 417–418 (2012) 10–19.
[38] C.G. De Kruif, Supra-aggregates of casein micelles as a prelude to coagulation, J. Dairy Sci. 81 (1998) 3019–3028.
[39] A. Bouchoux, G. Gésan-Guiziou, J. Perez, B. Cabane, How to squeeze a sponge: casein micelles under osmotic stress, a SAXS study, Biophys. J. 99 (2010) 3754–3762.
[40] P. Qu, A. Bouchoux, G. Gésan-Guiziou, On the cohesive properties of casein micelles in dense systems, Food Hydrocolloids 43 (2015) 753–762.
[41] F. Doudiès, A.-S. Arsène, F. Garnier-Lambrouin, M.-H. Famelart, A. Bouchoux, F. Pignon, G. Gésan-Guiziou, Major role of voluminosity in the compressibility and sol–gel transition of casein micelle dispersions concentrated at 7°C and 20°C, Foods 8 (2019) 652–671.
[42] A. Bouchoux, P.-E. Cayemitte, J. Jardin, G. Gésan-Guiziou, B. Cabane, Casein micelle dispersions under osmotic stress, Biophys. J. 96 (2009) 693–706.
[43] A. Bouchoux, B. Debbou, G. Gésan-Guiziou, M.-H. Famelart, J.-L. Doublier, B. Cabane, Rheology and phase behavior of dense casein micelle dispersions, J. Chem. Phys. 131 (2009), 165106.
[44] A. Bouchoux, P. Qu, P. Bacchin, G. Gésan-Guiziou, A general approach for predicting the filtration of soft and permeable colloids: the milk example, Langmuir 30 (2014) 22–34.
[45] L.K. Creamer, G.P. Berry, O.E. Mills, A study of the dissociation of β-casein from the bovine casein micelle at low temperature, N. Z. J. Dairy Sci. Technol. 12 (1977) 58–66.
[46] S. Nobel, K. Weidendorfer, J. Hinrichs, Apparent voluminosity of casein micelles determined by rheometry, J. Colloid Interface Sci. 386 (2012) 174–180.
[47] S. Nobel, C. Kern, A. Sonne, B. Bahler, J. Hinrichs, Apparent voluminosity of casein micelles in the temperature range 35-70°C, Int. Dairy J. 59 (2016) 80–84.
[48] C. David, F. Pignon, T. Narayanan, M. Sztucki, G. Gésan-Guiziou, A. Magnin, Spatial and temporal in-situ evolution of concentration profile during casein micelle ultrafiltration probed by small angle X-ray scattering, Langmuir 24 (2008) 4523–4529.
[49] Y. Jin, N. Hengl, S. Baup, F. Pignon, N. Gondrexon, M. Sztucki, G. Gésan-Guiziou, A. Magnin, M. Abyan, M. Karrouch, D. Bleses, Effects of ultrasound on cross-flow ultrafiltration of skim milk: characterization from macro-scale to nano-scale, J. Membr. Sci. 470 (2014) 205–218.
[50] Y. Jin, N. Hengl, S. Baup, G. Maitrejean, F. Pignon, Modeling and analysis of concentration profiles obtained by in-situ SAXS during cross-flow ultrafiltration of colloids, J. Membr. Sci. 528 (2017) 34–45.
[51] M.H. Famelart, F. Lepesant, F. Gaucheron, Y. Le Graet, P. Schuck, pH-induced physicochemical modifications of native phosphocaseinate suspensions: influence of aqueous phase, Lait 76 (1996) 445–460.
[52] C. Gaiani, J. Scher, P. Schuck, J. Hardy, S. Desobry, S. Banon, The dissolution behaviour of native phosphocaseinate as a function of concentration and temperature using a rheological approach, Int. Dairy J. 16 (2006) 1427–1434.
[53] C. Pompei, P. Resmini, C. Peri, Skim milk protein recovery and purification by ultrafiltration. Influence of temperature on permeation rate and retention, J. Food Sci. 38 (1973) 867–870.
[54] D.J. Kapsimalis, R.R. Zall, Ultrafiltration of skim milk at refrigerated temperatures, J. Dairy Sci. 64 (1981) 1945–1950.
[55] A. Makardij, X.D. Chen, M.M. Farid, Microfiltration and ultrafiltration of milk: some aspects of fouling and cleaning, Food Bioprod. Process. 77 (1999) 107–113.
[56] S.M.A. Razavi, S.M. Mousavi, S.A. Mortazavi, Dynamic prediction of milk ultrafiltration performance: a neural network approach, Chem. Eng. Sci. 58 (2003) 4185–4195.
[57] G. Samuelsson, P. Dejmek, G. Tragardh, M. Paulsson, Minimizing whey protein retention in cross-flow microfiltration of skim milk, Int. Dairy J. 7 (1997) 237–242.
[58] G. Samuelsson, I.H. Huisman, G. Tragardh, M. Paulsson, Predicting limiting flux of skim milk in crossflow microfiltration, J. Membr. Sci. 129 (1997) 277–281.
[59] N.D. Lawrence, S.E. Kentish, A.J. O'Connor, A.R. Barber, G.W. Stevens, Microfiltration of skim milk using polymeric membranes for casein concentrate manufacture, Separ. Purif. Technol. 60 (2008) 237–244.
[60] K. Karasu, N. Glennon, N.D. Lawrence, G.W. Stevens, A.J. O'Connor, A.R. Barber, S. Yoshikawa, S.E. Kentish, A comparison between ceramic and polymeric membrane systems for casein concentrate manufacture, Int. J. Dairy Technol. 63 (2010) 284–289.
[61] N.A. McCarthy, H.B. Wijayanti, S.V. Crowley, J.A. O'Mahony, M.A. Fenelon, Pilot-scale ceramic membrane filtration of skim milk for the production of a protein base ingredient for use in infant milk formula, Int. Dairy J. 73 (2017) 57–62.
[62] H.G.R. Rao, A.S. Grandison, M.J. Lewis, Flux pattern and fouling of membranes during ultrafiltration of some dairy products, J. Sci. Food Agric. 66 (1994) 563–571.
[63] M. Rabiller-Baudry, L. Begoin, D. Delaunay, L. Paugam, B. Chaufer, A dual approach of membrane cleaning based on physico-chemistry and hydrodynamics. Application to PES membrane of dairy industry, Chem. Eng. Process 47 (2008) 267–275.
[64] M. Leu, A. Marciniak, J. Chamberland, Y. Pouliot, L. Bazinet, A. Doyen, Effect of skim milk treated with high hydrostatic pressure on permeate flux and fouling during ultrafiltration, J. Dairy Sci. 100 (2017) 7071–7082.
[65] O. Le Berre, G. Daufin, Microfiltration (0·1 μm) of milk: effect of protein size and charge, J. Dairy Res. 65 (1998) 443–455.
[66] K. Schroen, A.M.C. Van Dinther, S. Bogale, M. Vollebregt, G. Brans, R.M. Boom, Membrane processes for dairy fractionation, in: K.-V. Peinemann, S. Pereira Nunes, L. Giorno (Eds.), Membranes for Food Applications, Wiley, Wageningen, 2010, pp. 25–43.
[67] H. Li, Y.-C. Hsu, Z. Zhang, N. Dharsana, Y. Ye, V. Chen, The influence of milk components on the performance of ultrafiltration/diafiltration of concentrated skim milk, Separ. Sci. Technol. 52 (2016) 381–391.
[68] M. Elimelech, S. Bhattacharjee, A novel approach for modeling concentration polarization in crossflow membrane filtration based on the equivalence of osmotic pressure model and filtration theory, J. Membr. Sci. 145 (1998) 223–241.
[69] R. Gebhardt, T. Steinhauer, P. Meyer, J. Sterr, J. Perlich, U. Kulozik, Structural changes of deposited casein micelles induced by membrane filtration, Faraday Discuss 158 (2012) 77–88.
[70] C. Rey, N. Hengl, S. Baup, M. Karrouch, A. Dufresne, H. Djeridi, R. Dattani, F. Pignon, Velocity, stress and concentration fields revealed by micro-PIV and SAXS within concentration polarization layers during cross-flow ultrafiltration of colloidal Laponite clay suspensions, J. Membr. Sci. 578 (2019) 69–84.
[71] C. Rey, N. Hengl, S. Baup, M. Karrouch, E. Gicquel, A. Dufresne, H. Djeridi, R. Dattani, Y. Jin, F. Pignon, Structure, rheological behavior, and in situ local flow fields of cellulose nanocrystal dispersions during cross-flow ultrafiltration, ACS Sustain. Chem. Eng. 7 (2019) 10679–10689.
[72] M. Loginov, F. Doudiès, N. Hengl, F. Pignon, G. Gésan-Guiziou, Influence of membrane resistance on swelling and removal of colloidal filter cake after filtration pressure release, J. Membr. Sci. 595 (2020), 117498.
[73] S. Obeid, F. Guyomarc'h, G. Tanguy, N. Leconte, F. Rousseau, A. Dolivet, A. Leduc, X. Wu, C. Cauty, G. Jan, F. Gaucheron, C. Lopez, The adhesion of homogenized fat globules to proteins is increased by milk heat treatment and acidic pH: quantitative insights provided by AFM force spectroscopy, Food Res. Int. 129 (2020), 108847.
[74] T. Tanaka, D.J. Fillmore, Kinetics of swelling of gels, J. Chem. Phys. 70 (1979) 1214–1218.
[75] G. Sudre, L. Olanier, Y. Tran, D. Hourdet, C. Creton, Reversible adhesion between a hydrogel and a polymer brush, Soft Matter 8 (2012) 8184–8193.
[76] S. Hong, R.S. Faibish, M. Elimelech, Kinetics of permeate flux decline in crossflow membrane filtration of colloidal suspensions, J. Colloid Interface Sci. 196 (1997) 267–277.
[77] H.C. Chua, T.C. Arnot, J.A. Howell, Controlling fouling in membrane bioreactors operated with a variable throughput, Desalination 149 (2002) 225–229.
[78] M.K. Jorgensen, K. Keiding, M.L. Christensen, On the reversibility of cake buildup and compression in a membrane bioreactor, J. Membr. Sci. 455 (2014) 152–161.
[79] R. Schopf, N. Schork, E. Amling, H. Nirschl, G. Guthausen, U. Kulozik, Structural characterisation of deposit layer during milk protein microfiltration by means of in-situ mri and compositional analysis, Membranes 10 (2020) 59.
[80] M.E. Weinberger, U. Kulozik, Effect of Low-Frequency Pulsatile Crossflow Microfiltration on Flux and Protein Transmission in Milk Protein Fractionation, Separation Science and Technology, Philadelphia, 2020, https://doi.org/10.1080/01496395.2020.1749080.
[81] M. Hartinger, J. Napiwotzki, E.-M. Schmid, F. Kurz, U. Kulozik, Semi-quantitative, spatially resolved analysis of protein deposit layers on membrane surfaces, Methods (Orlando) 7 (2020), 100780.
[82] M. Hartinger, H.-J. Heidebrecht, S. Schiffer, J. Dumpler, U. Kulozik, Technical concepts for the investigation of spatial effects in spiral-wound microfiltration membranes, Membranes 9 (2019) 80.
[83] M. Hartinger, S. Schiffer, H.-J. Heidebrecht, J. Dumpler, U. Kulozik, Investigation on the spatial filtration performance in spiral-wound membranes – influence and length-dependent adjustment of the transmembrane pressure, J. Membr. Sci. 591 (2019), 117311.
[84] D.J. McMahon, R.J. Brown, Composition, structure, and integrity of casein micelles: a review, J. Dairy Sci. 67 (1984) 499–512.
[85] D.G. Dalgleish, On the structural models of bovine casein micelles – review and possible improvements, Soft Matter 7 (2011) 2265–2272.
[86] D.G. Dalgleish, M. Corredig, The structure of the casein micelle of milk and its changes during processing, Annu. Rev. Food Sci. Tech. 3 (2012) 449–467.